

On dynamical network entropy in cancer

James West^{1,2}, Ginestra Bianconi³, Simone Severini^{2,4} and Andrew E Teschendorff^{1*}

¹Statistical Cancer Genomics, Paul O’Gorman Building, UCL Cancer Institute, University College London, 72 Huntley Street, London WC1E 6BT, United Kingdom.

²Department of Physics & Astronomy, University College London, London WC1E 6BT, United Kingdom.

³Department of Physics, Northeastern University, Boston, Massachusetts 02115, USA.

⁴Department of Computer Science, University College London, London WC1E 6BT, United Kingdom.

ABSTRACT

The cellular phenotype is described by a complex network of molecular interactions. Elucidating network properties that distinguish disease from the healthy cellular state is therefore of critical importance for gaining systems-level insights into disease mechanisms and ultimately for developing improved therapies. Recently, several statistical mechanical network properties have been studied in the context of cancer interaction networks, yet it is unclear which network properties best characterise the cancer phenotype. In this work we take a step in this direction by comparing two different types of molecular entropy in their ability to discriminate cancer from the normal phenotype. One entropy measure, called flux entropy, is dynamical in the sense that it is derived from a stochastic process satisfying an approximate diffusion equation over the cellular interaction network. The second measure, called covariance entropy, does not depend on the interaction network and is thus of a static nature. Using multiple gene expression data sets of normal and cancer tissue, encompassing approximately 500 samples, we demonstrate that flux entropy is a better discriminator of the cancer phenotype than covariance entropy. Specifically, we show that local flux entropy is always increased in cancer relative to normal tissue while the local covariance entropy is not. Furthermore, we show that gene expression differences between normal and cancer tissue are anticorrelated with local flux entropy changes, thus providing a systemic link between gene expression changes at the nodes and their local information flux dynamics. Finally, we show that genes located in the intracellular domain demonstrate preferential increases in flux entropy, while the dynamical entropy of genes encoding membrane receptors and secreted factors is preferential reduced. Thus, these results elucidate intrinsic network properties of cancer and support the view that the observed increased robustness of cancer cells to perturbation and therapy may be due to an increase in the dynamical network entropy that allows the cells to adapt to the new cellular stresses. Thus, using local flux entropy measures may also help identify novel drug targets which render cancer cells more susceptible to therapeutic intervention.

INTRODUCTION

The characterisation of cancer cells in terms of genetic (and epigenetic) aberrations has advanced our understanding of cancer biology, yet far fewer insights have been gained into systems-level properties that define the cancer cell phenotype. Since the normal physiological state of a cell is described by a complex interaction network, it makes sense to attempt identify systems-level properties of cancer by elucidating network properties that differentiate cancer from normal tissue. In line with this, the notion of “differential networks” has emerged, which attempts to better characterise disease phenotypes by studying the changes in interaction patterns (Taylor *et al.*, 2009; Hudson *et al.*, 2009; Teschendorff and Severini, 2010; Bandyopadhyay *et al.*, 2010; Califano, 2011; Ideker and Krogan, 2012), as opposed to merely analysing the changes in mean levels of some molecular quantity (e.g gene expression). As demonstrated by these studies (Taylor *et al.*, 2009; Hudson *et al.*, 2009; Teschendorff and Severini, 2010), differential networks can identify important gene modules implicated in cancer and also provide critical novel biological insights not obtainable using other approaches. This differential network strategy has recently received further impetus from studies of differential epistasis mapping in yeast, demonstrating that differential interactions may hold the key to understanding the systems-level responses of cells to exogenous and endogenous perturbations including those present in cancer cells (Bandyopadhyay *et al.*, 2010; Califano, 2011). However, from a systems-level perspective it is still very unclear what network properties best define the cancer cell phenotype. We propose that a better characterisation of these network properties is important, not only for a deeper understanding of cancer systems biology, but also for identifying novel drug targets and realizing the promise of personalized medicine. One popular and fruitful way to probe the changes in molecular interactions underpinning a genetic disease like cancer has been to integrate mRNA gene expression data of cancer and normal tissue with network models of protein interactions (Tuck *et al.*, 2006; Pujana *et al.*, 2007; Platzer *et al.*, 2007; Ulitsky and Shamir, 2007; Chuang *et al.*, 2007; Milanesi *et al.*, 2009; Taylor *et al.*, 2009; Hudson *et al.*, 2009; Nibbe *et al.*, 2010; Yao *et al.*, 2010; Komurov *et al.*, 2010; Komurov and Ram, 2010; Teschendorff and Severini, 2010; Schramm *et al.*, 2010; Vazquez, 2010). The integration has

*to whom correspondence should be addressed

been performed at the level of proteins whereby gene expression values are overlaid onto the nodes of the network (see e.g. Ulitsky and Shamir (2007); Chuang *et al.* (2007)), and at the level of protein-interactions whereby weights are assigned to the edges according to the expression correlation strength (see e.g. Taylor *et al.* (2009)). Recently, several studies have started to investigate the statistical properties of these integrated weighted networks (Taylor *et al.*, 2009; Teschendorff and Severini, 2010; Schramm *et al.*, 2010; Komurov and Ram, 2010). In fact, from the correlations in gene expression a natural random walk process on these networks can be defined by a stochastic “flux” matrix, p_{ij} , which reflects the probability of diffusion along any given edge $i \rightarrow j$ in the network. From this local stochastic matrix one may then define for each gene (i.e. node i) in the network a local flux entropy,

$$S_i \propto - \sum_{j \in N(i)} p_{ij} \log p_{ij} \quad (1)$$

where $N(i)$ denotes the neighbors of gene i in the network (Teschendorff and Severini, 2010). We previously showed that primary tumours that metastasize exhibit an increase in this local entropy compared to primary tumours that do not spread (Teschendorff and Severini, 2010). Moreover, we showed that the increases in local flux entropy affected many genes in known tumour suppressor pathways, supporting the view that this increased dynamical disorder is caused by the higher frequency of genomic alterations underlying the metastatic phenotype.

The purpose of the present study is three-fold. First, to extend our previous investigation by exploring the changes in flux entropy between normal and cancer tissue. Second, to extend the notion of local flux entropy to a non-local/global one, i.e. for subnetworks. Third, to determine if the observed changes in flux entropy in cancer are dependent on the underlying interaction network and network dynamics.

To address the first question, we collected and analysed the largest available gene expression data sets encompassing relatively large numbers of both normal and cancer tissue, thus allowing for an objective comparison between phenotypes. To address the second problem we consider a diffusion process over the graph (Barrat *et al.*, 2008) and define a non-local flux entropy from a stochastic matrix that satisfies an approximate diffusion equation over the network. This construction is therefore closely related to the heat kernel PageRank algorithm (Chung, 2007; Brin and Page, 1998; Barrat *et al.*, 2008). To address the third question, we consider a different type of molecular entropy, called covariance entropy, which merely reflects the similarity of gene expression profiles (van Wieringen and van der Vaart, 2011). In fact, while flux entropy is derived from a stochastic matrix, the covariance entropy is defined from the symmetric covariance matrix and therefore lacks a dynamical interpretation in terms of diffusion or random walks. Hence, by comparing these different types of molecular entropy, we can study how relevant the network dynamics is for the characterisation of the cancer phenotype.

METHODS

The protein interaction network (PIN)

We downloaded the complete human protein interaction network from Pathway Commons (www.pathwaycommons.org) (Jan.2011) (Cerami *et al.*, 2011), which brings together protein interactions from several distinct sources. We then built a reduced protein interaction network from integrating the following sources: the Human Protein Reference Database (HPRD) (Prasad *et al.*, 2009), the National Cancer Institute Nature Pathway Interaction Database (NCI-PID) (pid.nci.nih.gov), the Interactome (Intact) (<http://www.ebi.ac.uk/intact/>) and the Molecular Interaction Database (MINT) (<http://mint.bio.uniroma2.it/mint/>). Protein interactions in this network include physical stable interactions such as those defining protein complexes, as well as transient interactions such as post-translational modifications and enzymatic reactions found in signal transduction pathways, including 20 highly curated immune and cancer signaling pathways from NetPath (www.netpath.org) (Kandasamy *et al.*, 2010). We focused on non-redundant interactions, only included nodes with an Entrez gene ID annotation and focused on the maximally connected component, resulting in a connected network of 10,720 nodes (unique Entrez IDs) and 152,889 documented interactions. In what follows we refer to this network as the “PIN”.

Normal and cancer tissue gene expression data sets

We searched Oncomine (Rhodes *et al.*, 2004) for studies which (i) had profiled reasonable numbers of cancer and normal tissue samples (at least ~ 25 of each type), and (ii) which had been profiled on an Affymetrix platform. In order to reliably estimate covariance of two genes across a set of samples, at least ~ 25 samples are needed. The second criterion reflects the desire to conduct the study on a common platform and Affymetrix arrays are the most widely used. Using the same platform across studies ensured that the integrated mRNA-PIN networks were of similar size. In all cases, the intra-array normalised data was downloaded from GEO (www.ncbi.nlm.nih.gov/geo/), quantile normalized, and subsequently probes mapping to the same Entrez gene ID were averaged. We then subjected each study that passed these criteria through a quality control step, which involved a Principal Component Analysis (PCA) to check that (iii) the dominant component of variation correlated with cancer/normal status. If not, this indicated to us a more pronounced source of non-biological variation, which would confound our downstream analysis. There were six studies satisfying all three criteria and the tissues profiled included bladder (48 normals and 81 cancers) (Sanchez-Carbayo *et al.*, 2006), lung (49 normals and 58 cancers) (Landi *et al.*, 2008), gastric (31 normals and 38 cancers) (D’Errico *et al.*, 2009), pancreas (39 normals and cancers) (Badea *et al.*, 2008), cervix (24 normals and 33 cancers) (Scotto *et al.*, 2008) and liver (23 normals and 35 cancers) (Wurmbach *et al.*, 2007).

Integrated PIN-mRNA expression networks and the stochastic information flux matrix

For a given cellular phenotype (i.e. cancer or normal), we build an integrated mRNA-PIN using the same procedure as described in (Teschendorff and Severini, 2010). Briefly, edge weights in the PIN

were defined by a stochastic matrix p_{ij} ,

$$p_{ij} = \frac{w_{ij}}{\sum_{k \in \mathcal{N}(i)} w_{ik}} \quad (2)$$

with $\sum_{j \in \mathcal{N}(i)} p_{ij} = 1$, where $\mathcal{N}(i)$ denotes the neighbors of gene i in the PIN and where $w_{ij} = \frac{1}{2}(1 + C_{ij})$ denotes the transformed Pearson correlation coefficient C_{ij} of gene expression between genes i and j across the samples belonging to the given phenotype. This definition of w_{ij} reflects our desire to treat correlations and anti-correlations differently. We also note that we enforce $p_{ij} = 0$ whenever (i, j) is not an edge in the PIN. Thus, the integrated mRNA-PINs with the edge weights as defined by p_{ij} , can be viewed as approximate models of signal transduction flow (as measured by positive gene-gene correlations in expression) subject to the structural constraint of the PIN. Applying this procedure to the two phenotypes yields two integrated PIN-mRNA networks, one for the cancer phenotype with stochastic matrix $p_{ij}^{(C)}$, and one for the normal phenotype with stochastic matrix $p_{ij}^{(N)}$.

It is important to stress that we have approximated signal transduction flux on the PIN by positive correlations in expression between interacting genes. This is obviously a crude approximation and therefore a limitation of this study, however, until other types of matched molecular data (e.g protein expression, phosphorylation and other post-translational modification states) become available on a genome-wide basis, we are restricted to the use of only gene expression data. Nevertheless, some important rationale and justification for the use of gene expression correlations to approximate signaling flux over the network will be provided by careful comparison of the local correlations to those which are non-local.

A heat kernel stochastic matrix

It is clear that the stochastic matrix p_{ij} above defines a (biased) random walk on the network \mathcal{N} . One may thus compute an information (or probability) flux between any two nodes i and j in \mathcal{N} (Estrada and Rodriguez-Velazquez, 2005). In fact, it is clear that the probability flux of moving from i to j over a path of length L is given by $(p^L)_{ij}$. It follows that the total probability flux E_{ij} between i and j is given by

$$E_{ij} = \gamma \sum_{L=1}^{\infty} \alpha_L (p^L)_{ij} \quad (3)$$

where γ is a normalisation factor and where we have introduced a set of arbitrary weights α_L to allow variable contributions for paths of different lengths. One possibility is to suppress paths of longer lengths using $\alpha_L = 1/L!$, which also guarantees convergence of the infinite series (Estrada and Rodriguez-Velazquez, 2005). Formally, defining $\alpha_L = t^L/L!$, we obtain the stochastic matrix

$$K_{ij}(t) = \frac{\sum_{L=1}^{\infty} \frac{t^L}{L!} (p^L)_{ij}}{e^t - 1} \quad (4)$$

where we have introduced a ‘‘temperature’’ parameter t (Chung, 2007). This stochastic matrix is a modified version of the heat-kernel

stochastic matrix (Chung, 2007) and satisfies

$$\partial_t K(t) = -K(t)(I - p) + \frac{p - K(t)}{e^t - 1} \quad (5)$$

where we have suppressed matrix indices and where I denotes the identity matrix. Since $p_{ij}, K_{ij}(t) \leq 1 \forall i, j, t$, it follows that for sufficiently large temperatures ($t \geq 1$), $K(t)$ approximates a solution of the heat-diffusion equation (Chung, 2007)

$$\partial_t K(t) \approx -K(t)(I - p) \quad (6)$$

Thus, the choice $\alpha = t^L/L!$ leads to a natural interpretation in terms of a discrete approximate diffusion process on a graph (Barrat *et al.*, 2008).

The information flux entropy

Given the matrix K_{ij} , let Q denote the number of non-zero K_{ij} , i.e. $Q = \sum_{ij} I(K_{ij} > 0)$ where I is here the indicator function. We then define an information flux entropy as

$$S_{\mathcal{N}}(t) = -\frac{1}{\log Q} \sum_{ij} K_{ij}(t) \log K_{ij}(t) \quad (7)$$

where we have rescaled $K_{ij}(t)$ by $1/n$ in order to ensure that $\sum_{ij} K_{ij}(t) = 1$. Note that the information flux entropy defined above can be thought of as a non-equilibrium entropy, since the stationary distribution π_i of K_{ij} , defined by $\pi_i K_{ij} = \pi_j$, was not included. Our choice to consider this non-equilibrium version is motivated by our desire to objectively compare the flux entropy to the covariance entropy, which does not have a stationary distribution, as explained in the next subsection.

Suppose now that we consider diffusion/flux over paths of maximum length 1. Then, this leads to $K_{ij} = p_{ij}/n$ where n is the number of nodes in \mathcal{N} (we have set $t = 1$ for convenience). This leads to the expression

$$\begin{aligned} S_{\mathcal{N}}^{(1)} &= \frac{1}{\log Q} \left\{ -\frac{1}{n} \sum_{ij} p_{ij} \log p_{ij} + \log n \right\} \\ &= \frac{1}{\log Q} \left\{ \frac{1}{n} \sum_i S_i \log k_i + \log n \right\} \end{aligned}$$

In the above expression, S_i is the local flux entropy of node i (Barrat *et al.*, 2008; Teschendorff and Severini, 2010),

$$S_i = -\frac{1}{\log k_i} \sum_{j \in \mathcal{N}(i)} p_{ij} \log p_{ij} \quad (8)$$

where k_i is the degree of node i and the normalisation factor ensures that the maximum attainable entropy is equal to 1, independent of the degree of the node.

Next, we can consider flux over paths up to length two, in which case

$$K_{ij}^{(2)} = \frac{p_{ij} + \frac{1}{2}(p^2)_{ij}}{\frac{3}{2}n} \quad (9)$$

and the corresponding entropy,

$$S_{\mathcal{N}}^{(2)} = -\frac{1}{\log Q} \sum_{ij} K_{ij}^{(2)} \log K_{ij}^{(2)} \quad (10)$$

In principle, we can estimate the flux entropy $S^{(h)}$ for paths of arbitrary order h . In this case,

$$K_{ij}^{(h)} = \frac{1}{n \sum_{r=1}^h \frac{1}{r!}} \left(\sum_{r=1}^h \frac{1}{r!} (p^r)_{ij} \right) \quad (11)$$

In this work we compute flux entropies up to moments of order 5 using the R-package *expm*. Not going beyond $h = 5$ is justified for two reasons: (i) the most interesting behaviour is found for $h \leq 3$, (ii) the computational cost for $h = 5$ is considerable, for instance, estimation of flux entropy and associated sampling variance estimates for a typical data set of 30 samples and ~ 7500 nodes at $h = 5$ takes at least ~ 20 hours on a high-performance quad processor workstation.

The covariance entropy

In addition to the information flux entropy, we also consider a different type of entropy which merely quantifies the degree of similarity of gene expression profiles (as determined by Pearson correlations). Given a set of p genes (i.e. the vertices of our PIN or a subgraph thereof) with mean expression vector $\mu = (\mu_1, \dots, \mu_p)$ and $p \times p$ covariance matrix Σ , both computed over the samples within a given phenotype, its covariance entropy, S^Σ , is given by (van Wieringen and van der Vaart, 2011)

$$\begin{aligned} S^\Sigma &= \frac{1}{2} \log \det \Sigma + \frac{1}{2} p (1 + \log 2\pi) \\ &= \frac{1}{2} \sum_i \log \lambda_i + \frac{1}{2} p (1 + \log 2\pi) \end{aligned}$$

assuming multivariate normality of the expression matrix. Since typically $p > n_s$ (n_s = number of samples in the given phenotype), the eigenvalues λ_i of the covariance matrix need to be estimated using a shrinkage estimator (Schaefer and Strimmer, 2005). This approximation for the entropy was shown to be in good agreement with non-parametric estimators (van Wieringen and van der Vaart, 2011). When estimating the covariance matrix we would allow for any pairwise gene covariances, which therefore does not take the network structure into account. To obtain local estimates of covariance entropy which do take the local network neighborhood into account, we compute a covariance entropy for each node $i \in \mathcal{N}$ as,

$$S_i^\Sigma = \frac{1}{2} \log \det \Sigma_{i \cup \mathcal{N}(i)} + \frac{1}{2} (k_i + 1) (1 + \log 2\pi) \quad (12)$$

where $\Sigma_{i \cup \mathcal{N}(i)}$ is the covariance matrix over the subgraph $i \cup \mathcal{N}(i)$, i.e. the subgraph made up of node i and its neighbours $\mathcal{N}(i)$. In this case, a shrunken estimate of the covariance matrix is only needed for nodes with degrees $k_i > n_s - 1$. Using a different estimator for the covariance matrix depending on the degree of the nodes is justified since we are interested in making comparisons between the normal and cancer networks and the node degrees are unchanged between the two phenotypes.

Since we are interested in studying the changes in correlative patterns between phenotypes we estimate the covariance entropies from a rescaled expression matrix where each feature (gene) has a unit variance over the specific phenotype. This then guarantees that

$\Sigma_{ii} = 1 \quad \forall i = 1, \dots, p$. Under these constraints and for fixed p , the maximum possible covariance entropy corresponds to the case when $\Sigma = I$, i.e. when the covariance matrix is the identity matrix. The maximum covariance entropy value is then $\frac{1}{2} p (1 + \log 2\pi)$. Thus, to ensure that the maximum value is independent of p we divide the above definition of local covariance entropy by the maximum attainable value, so that $S_i^\Sigma \leq 1 \quad \forall i$.

Sampling variance using the jackknife

To estimate the statistical significance of observed differences in entropy between two phenotypes, we decided to use the jackknife procedure (Wu, 1986). Briefly, the jackknife procedure removes one sample at a time from the given phenotype and recomputes the desired quantity S (here entropy). Thus, if there are n samples in the given phenotype one obtains n jackknife estimates ($\hat{S}_{J,j} : j = 1, \dots, n$). A jackknife estimate for the mean S_μ and variance S_V of S is then obtained as

$$\begin{aligned} \hat{S}_\mu &= n\hat{S} - (n-1)\langle \hat{S}_{J,j} \rangle_j \\ \hat{S}_V &= \frac{n-1}{n} \sum_{j=1}^n (\hat{S}_{J,j} - \langle \hat{S}_{J,j} \rangle_j) \end{aligned}$$

where \hat{S} is the estimate using all n samples and $\langle \hat{S}_{J,j} \rangle_j = \frac{1}{n} \sum_{j=1}^n \hat{S}_{J,j}$. Thus, for two phenotypes ‘‘N’’ and ‘‘C’’, we compute the difference $\Delta S_J = \hat{S}_\mu^{(C)} - \hat{S}_\mu^{(N)}$ and obtain a z-statistic

$$z = \frac{\Delta S_J}{\sigma_J} \quad (13)$$

where $\sigma_J = \sqrt{S_V^{(N)} + S_V^{(C)}}$.

This jackknife procedure can be applied to both flux and covariance entropy defined over the network or for each node. Note that in the case where we obtain z-statistics for each gene/node, the genes can then be ranked according to the significance of this z-statistic.

It should be pointed out that although bootstrapping provides an alternative to the jackknife, that it is not appropriate here since the resampling with replacement would artificially inflate correlations (van Wieringen and van der Vaart, 2011). Another procedure, adopted in (van Wieringen and van der Vaart, 2011), could be to permute the phenotype labels, so that a given ‘‘permuted’’ phenotype contains now a mixture of ‘‘normals’’ and ‘‘cancers’’. However, because there are massive differences in expression between normal and cancer, this procedure would dramatically alter the distribution of correlations within the new permuted phenotypes which would also not yield the correct null distribution. Thus, the jackknife strategy circumvents this difficulty while also avoiding the bias associated with bootstrapping.

RESULTS

We identified six expression data sets encompassing sufficient numbers of normal and cancer tissue samples and which passed our quality control criteria (Methods). The tissues profiled were bladder, lung, stomach, pancreas, cervix and liver. Integration of these expression data sets with our protein interaction network (PIN) (Methods) yielded sparse weighted networks of approximately 7500 nodes and 98500 edges. The average degree, median degree and

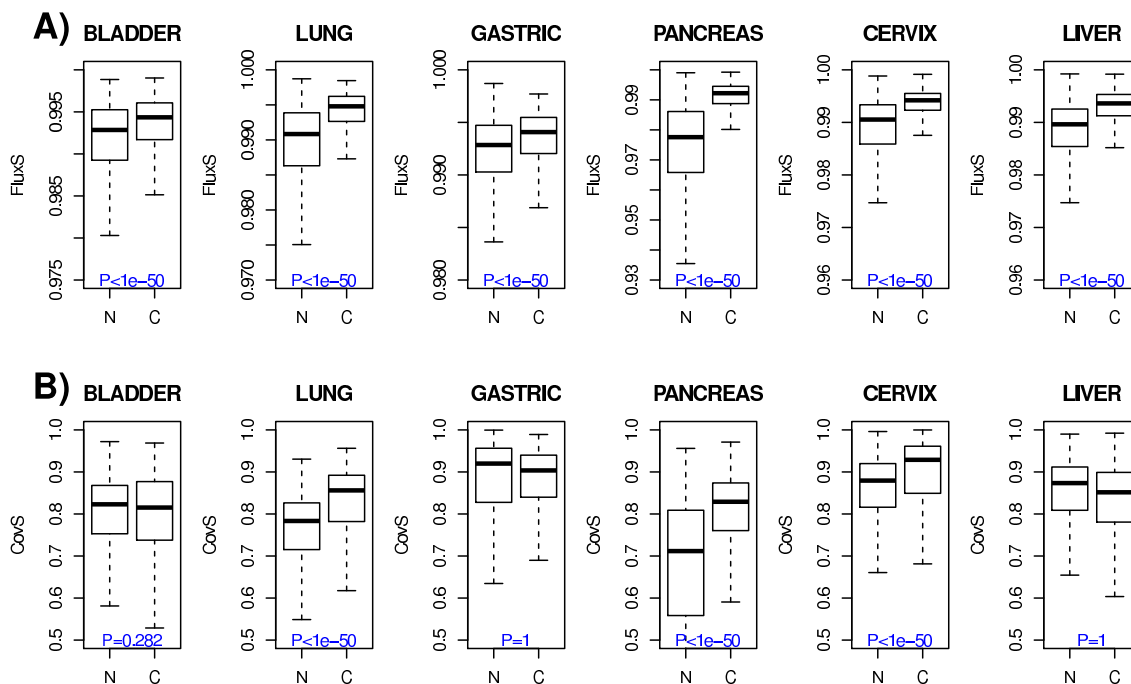


Fig. 1. **A)** Boxplots of local (i.e. per node) flux entropies (y-axis, FluxS) in cancer (C) and normal (N) tissue for all nodes with degree ≥ 10 (~ 3500 nodes) and across the six different tissue types. P-values are from a one-tailed unpaired Wilcoxon rank sum test. **B)** As A) but for the local covariance entropies (CovS). Both flux and covariance entropies have been normalised so that the maximum attainable value is 1.

diameter of these integrated networks were approximately 26, 8 and 12, respectively. An important assumption underlying any analysis on these integrated networks is that genes which are neighbors in the network are more likely to be correlated at the level of gene expression. While this has been shown for specific data sets (see e.g Taylor *et al.* (2009)), we verified that it also holds for the integrated mRNA-PIN networks considered here (Fig.S1).

Increased information flux entropy as an intrinsic property of the cancer cell phenotype

We previously showed that primary breast cancers that metastasize exhibit an increased flux entropy compared to breast cancers that do not spread (Teschendorff and Severini, 2010). Comparing distinct cancer phenotypes to each other has the advantage of having access to larger sample sizes, thus allowing for more reliable estimates of expression correlations. Nevertheless we here sought to determine if flux entropy also discriminates cancer from its respective normal tissue phenotype. A comparison of the distributions of local flux entropies between normal and cancer across six different tissue types confirmed that cancer is indeed characterised by an increased flux entropy (Fig.1A).

To investigate if the specific network dynamics is important in characterising the cancer phenotype, we computed a local covariance entropy (Methods). While the local covariance entropy also takes the neighborhood of each node into account, it is derived from a covariance matrix and therefore does not admit a dynamical interpretation. Interestingly, and in contrast to flux entropy, local covariance entropies were not always significantly higher in cancer (Fig.1B). In fact, in 3 out of 6 tissues, covariance entropies were lower in cancer (Fig.1B). The statistics of differential

entropy between cancer and normal, derived from an unpaired non-parametric test, were also higher for local flux entropy than local covariance entropy (Table 1). The higher discriminatory power of flux entropy was retained when a paired non-parametric test was used to account for potential dependencies between the normal and cancer entropies at each node (Table 1).

Thus, these results indicate that the specific network dynamics considered is of relevance for characterising the cancer phenotype. Indeed, only flux entropy provided a consistent discriminator between the normal and cancer phenotypes, and moreover, the power of discrimination was also consistently higher for flux entropy. Thus, the increased dynamical disorder appears to be an intrinsic property of the cancer cell phenotype.

Higher order non-local flux entropy

Given that local flux entropy can discriminate the cancer and normal phenotypes, it is natural to ask if higher order flux entropies, computed over paths of length larger than 1, are also discriminatory. To this end, we computed for the normal and cancer phenotypes, a higher-order flux entropy

$$S_N^{(2)} \propto - \sum_{ij} K_{ij}^{(2)} \log K_{ij}^{(2)} \quad (14)$$

where $K_{ij}^{(2)}$ satisfies an approximate diffusion equation over the network (Methods). We point out that even when i and j are neighbors, that $K_{ij}^{(2)}$ is not equal to p_{ij} , since we allow for alternative signaling paths (of maximum length 2) between genes i and j . Thus, this flux entropy also takes the well-known redundancy of signaling paths into account (Tier *et al.*, 2010). We observed

Table 1. Wilcoxon rank sum test statistics comparing the flux entropies (FluxS) and covariance entropies (CovS) between normal and cancer, and across the six tissue types. We provide statistics for both the unpaired and paired (i.e. treating the cancer and normal entropies for each gene as dependent variables) version of Wilcoxon rank sum tests. The test-statistics are one-tailed (hypothesis is that cancer has higher entropy) and have been normalised to lie between 0 and 1. Values close to 0.5 and less than 0.5 mean no discrimination and higher entropy in normal phenotype, respectively, while values closer to 1 indicate significantly higher entropy in cancer.

| | BLAD. | LUNG | GAST. | PANC. | CERV. | LIV. |
|-----------------|-------|------|-------|-------|-------|------|
| UNPAIRED | | | | | | |
| FluxS | 0.61 | 0.76 | 0.61 | 0.87 | 0.76 | 0.76 |
| CovS | 0.50 | 0.73 | 0.45 | 0.75 | 0.66 | 0.44 |
| PAIRED | | | | | | |
| FluxS | 0.75 | 0.92 | 0.69 | 0.97 | 0.88 | 0.88 |
| CovS | 0.57 | 0.86 | 0.56 | 0.99 | 0.75 | 0.49 |

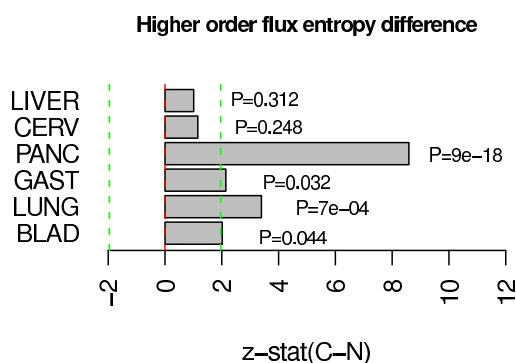


Fig. 2. z-statistics of differential non-local flux entropy (x-axis) for the six different tissues (y-axis). The flux entropy considered here is the $S^{(2)}$ measure which is defined for a stochastic diffusion matrix for maximum path lengths of order 2 (Methods). Positive z-statistics means higher entropy in cancer compared to normal. Green lines indicate the 95% confidence interval envelope and given P-values are from a normal null distribution centred at zero.

a higher flux entropy in cancer compared to normal tissue across all tissue types, although this was only statistically significant for the four larger studies (Fig.2). We also computed higher order entropies up to paths of maximum length 5. However, as with $S^{(2)}$, higher order flux entropies $S^{(k)}$, $k \geq 3$ generally exhibited reduced discriminatory power (data not shown), suggesting that the interesting dynamical changes associated with flux entropy in cancer are localised to neighbors and nearest neighbors in the interaction network.

Relation between differential expression and differential entropy

Our underlying biological hypothesis is that genes which exhibit an increase in local flux entropy do so because they become inactivated in cancer. Thus, one would expect tumour suppressor genes to show preferential increases in flux entropy. Conversely,

Table 2. Relation between differential expression and differential flux entropy (FluxS), and between differential expression and differential covariance entropy (CovS). The odds ratio (OR) reflects the odds of a gene overexpressed in cancer showing reduced (flux/covariance) entropy in cancer, compared to a gene that is underexpressed. The P-value (P) reflects the statistical significance of the odds ratio.

| | BLAD. | LUNG | GAST. | PANC. | CERV. | LIV. |
|--------------|-------|------|-------|--------|-------|-------|
| FluxS | | | | | | |
| OR | 6.24 | 3.07 | 2.43 | 2.17 | 3.64 | 2.80 |
| P | 3e-9 | 0.04 | 0.05 | 0.03 | 0.02 | 0.005 |
| CovS | | | | | | |
| OR | 1.24 | 0.73 | 2.49 | < 0.01 | 0.85 | 3.70 |
| P | 0.09 | 0.91 | 6e-6 | 1 | 0.76 | 2e-12 |

one would expect genes that become activated in cancer (e.g. oncogenes) to exhibit preferential reductions in entropy since the activation is likely to lead to the subsequent activation of an associated signalling pathway, possibly mediated by one of the neighbors of the oncogene. While the activation/inactivation of oncogenes/tumour suppressors is caused by underlying genetic and epigenetic alterations, the specific alteration patterns are not available for the tumours considered here. However, since the effects of these alterations are mediated by the corresponding changes in gene expression we can directly test the hypothesis in relation to the directional changes in gene expression between normal and cancer tissue. Thus, for each gene we computed a regularized t-statistic (Smyth, 2004) that reflects the degree of differential expression between normal and cancer tissue. Similarly, for each gene we used jackknife estimates to derive a z-statistic that reflects the degree of differential entropy between the normal and cancer phenotype (Methods). Next, we selected those genes with significant changes in both differential expression and differential flux entropy ($P < 0.05$). Confirming our hypothesis, we observed that genes significantly overexpressed in cancer showed preferential reductions in flux entropy compared to genes which were underexpressed, and the associated odds ratios were statistically significant across all 6 tissue types (Table 2). In contrast, this anticorrelation was only observed in 2 of the 6 tissues when the covariance entropy was considered (Table 2), further supporting the view that the flux dynamics defined on the networks is meaningful and that changes in the local flux dynamics around nodes reflect the underlying changes in gene expression at these nodes.

Differential local entropy correlates with the signaling domain of genes

It is of interest to explore the pattern of differential local entropy in relation to the topological properties and location of the genes in the interaction network. Dividing up the genes in the network into date-hubs, party-hubs (hub-bottlenecks), nonhub bottlenecks and nonhub-nonbottlenecks using a definition similar to that used in (Yu et al., 2007) showed that hubs exhibited only marginally larger changes in flux entropy (Wilcoxon rank sum test $P = 0.04$). However, by dividing up the genes in the

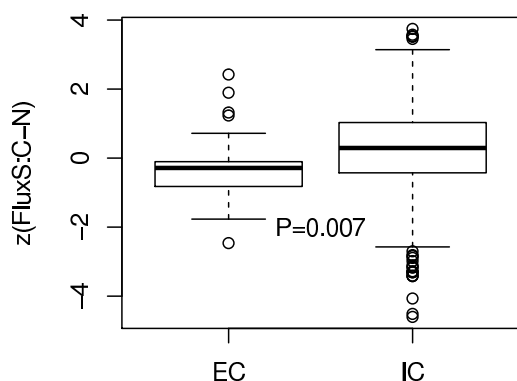


Fig. 3. The statistics of differential local flux entropy change (y-axis) against the main signaling domain (EC:extracellular/membrane receptor, IC:intracellular/nuclear) in the bladder cancer set. The P-value is from a two-tailed Wilcoxon rank sum test.

network into the two major extracellular/membrane (EC) and intracellular/nuclear (IC) signaling domains (Komurov and Ram, 2010), we observed a significantly different pattern of differential local entropy, with genes mapping to the intracellular domain demonstrating preferential increases in flux entropy, while gene encoding membrane receptors and secreted factors exhibited preferential decreases (Fig.3). However, we note that some genes in the intracellular domain also exhibited marked reductions in flux entropy.

Differential flux entropy captures dynamical changes in the cell-cycle and not stromal variations

The observed dependence of differential entropy patterns on the signaling domain supports the view that most of these patterns are due to signaling changes in the epithelial tumour cells, and we posited that the small number of intra-cellular genes showing significant entropy decreases (Fig.3) could reflect the increased activity of the cell-cycle in cancer. We thus performed a gene set enrichment analysis using the Molecular Signatures Database (MSigDB, (Subramanian *et al.*, 2005)) on the top ranked genes, ranked according to the magnitude of differential flux entropy (separately for increased and reduced entropy). In doing so, we also sought to determine the role, if any, that changes in immune and stromal cell composition could have. To this end we constructed a set of well known cell differentiation and surface markers from MSigDB. Confirming our hypothesis, genes implicated in the cell-cycle showed statistically significant reductions in flux entropy across most of the studies (Table 3). In contrast, cell differentiation markers were generally not enriched and only showed a more marginal trend towards lower flux entropy in cancer, also consistent with cancers exhibiting a somewhat higher level of immune/stromal cell infiltration. Together, these results indicate that flux entropic changes are capturing mostly changes in the intracellular wiring of the tumour epithelial cells.

Table 3. Enrichment analysis of cell differentiation (Cell-Diff.) markers and cell-cycle genes among the top 10% ranked genes exhibiting entropy increases (C>N) and decreases (N>C). The enrichment odds ratio (OR) and P-value (P) is from a one-tailed Fisher exact test. NA=not available due to insufficient number among the top 10%.

| | BLAD. | LUNG | GAST. | PANC. | CERV. | LIV. |
|-------------------|-------|-------|-------|-------|-------|-------|
| CELL-DIFF. | | | | | | |
| FluxS(C>N) | | | | | | |
| OR | 0.50 | 0.47 | 0.79 | 0.88 | 1.22 | 0.77 |
| P | 0.95 | 0.98 | 0.76 | 0.69 | 0.30 | 0.79 |
| FluxS(N>C) | | | | | | |
| OR | 1.36 | 14.12 | 1.44 | NA | 2.74 | 1.24 |
| P | 0.30 | 0.01 | 0.23 | NA | 0.11 | 0.44 |
| CELL-CYCLE | | | | | | |
| FluxS(C>N) | | | | | | |
| OR | 0.44 | 0.72 | 1.13 | 0.50 | 1.04 | 0.50 |
| P | 0.99 | 0.93 | 0.36 | 0.99 | 0.46 | 0.99 |
| FluxS(N>C) | | | | | | |
| OR | 3.92 | 6.07 | 1.35 | NA | 2.62 | 6.61 |
| P | 2e-8 | 0.07 | 0.17 | NA | 0.04 | 4e-11 |

DISCUSSION

In this study we have performed a detailed comparison of molecular entropy metrics in cancer and have in the process elucidated a system-omic principle underlying cancer. By defining a dynamics of information flux on a network of protein interactions, we have shown that entropy associated with this dynamics is increased in the cancer phenotype. Importantly, in the absence of this network dynamics, the molecular entropy does no longer provide a consistent discriminator of the cancer phenotype. This is an important insight, because it shows that the specific network dynamics considered has a biological meaning of relevance to cancer.

It is of importance to discuss (i) what may cause cancer cells to exhibit this increase in dynamical entropy and (ii) what it may mean for the cancer phenotype itself. Concerning the first question, one would expect genes that become inactivated in cancer to represent foci of increased flux entropy since the inactivation compromises its biological function: at the level of mRNA expression this would manifest itself as reduced expression correlations with its interacting neighbors, but more generally as an increased uncertainty as to which neighbors it may interact with. Conversely, for a gene that is overactivated in cancer its biological function is enhanced leading to an increased flux of the associated oncogenic pathway. In terms of local flux entropy this increased flux along a particular path in the network corresponds to a reduced uncertainty along which path the information is transferred. In line with these biological expectations we did observe that genes overexpressed in cancer were significantly more likely to exhibit reductions in flux entropy than underexpressed genes. Interestingly, this anticorrelation between local differential expression and entropy was more consistent (across studies) for flux entropy than covariance entropy, further suggesting that the network dynamics is biologically meaningful and that changes in this dynamics reflect the underlying changes in gene expression. It will be interesting to test these hypotheses further using multidimensional cancer

genomic profiles that encompass mutational, DNA methylation, copy-number and mRNA expression profiles for the same tumours (see e.g TCGA (2011)), although an objective comparison will require equal numbers of normal tissue samples, which for most cancers is not yet available (TCGA, 2011). However, already supporting the biological and clinical relevance of our flux entropy measure, we indeed observed that many of the genes exhibiting the largest reductions in entropy were either known or candidate oncogenes. For instance we observed *AURKB* to be the most highly ranked gene in bladder cancer. Given the well established oncogenic role of *AURKA* in bladder cancer (see e.g Park *et al.* (2008)), our analysis therefore suggests that the closely related kinase, *AURKB*, which has already been implicated as an oncogene and potential drug target in other cancers (Lens *et al.*, 2010; Lucena-Araujo *et al.*, 2011; Morozova *et al.*, 2010), may also play an equally important role in the pathogenesis of bladder cancer.

It will also be interesting to explore the changes in the network dynamics, including flux entropy, in the context of the different types of network motifs (Cui *et al.*, 2007). At this stage we can only speculate that the observed global increase in flux entropy reflects a higher frequency of inactivating over activating alterations in cancer. Intuitively, one would expect cancer cells to be characterised by many more inactivating changes since a random mutation/alteration is more likely to inactivate than activate a gene, and indeed this would be in agreement with recent reports suggesting that most genetic alterations are inactivating and affect tumour suppressors (Wood *et al.*, 2007). Supporting this further, we have seen that the preferential increase in flux entropy was observed mainly for genes in the intracellular domain, consistent with the evidence that most of the genetic and epigenetic alterations affect genes in this signaling domain (Forbes *et al.*, 2011).

Concerning the second question posed above, we propose that the increased flux entropy in cancer may endow cancer cells with the flexibility to adapt to the strong selective pressures of the tumour microenvironment. Moreover, the increased flux entropy could underpin the intrinsic robustness of cancer cells to endogenous and exogenous perturbations, including therapeutic intervention. Indeed, a general fluctuation theorem from statistical mechanics (Manke *et al.*, 2005, 2006) states that changes in network (topological) entropy, ΔS , and robustness, ΔR , are correlated, i.e

$$\Delta S \Delta R > 0 \quad (15)$$

Thus, according to this theorem if a node associated with high network entropy is removed, i.e if $\Delta S < 0$, then $\Delta R < 0$, meaning that the network is less robust as a result of this perturbation. In the context of our dynamical entropy and in comparing normal to cancer tissue, we are interested in those genes which show the largest changes in differential flux entropy. Thus, cancer alterations that lead to significant increases in flux entropy may contribute to the dynamical robustness of these cancer cells, whilst those alterations that are associated with reductions in flux entropy may make these cells less dynamically robust. Interestingly, this would fit in well with one of the important cancer hallmarks, namely, that of oncogene addiction, whereby cancer cells become overly reliant on a specific oncogenic pathway (Hanahan and Weinberg, 2011). In the case that the activated oncogene is druggable (e.g *ERBB2* in breast cancer), targeting of this oncogene has proved to be an effective drug therapy strategy (Hanahan and Weinberg, 2011).

However, the most common scenario is one where the oncogene is not directly druggable. Thus, in these cases it may be possible to use differential flux entropy to identify (neighboring) viable drug targets that also exhibit significant reductions in flux entropy. This novel computational strategy could therefore guide non-oncogene addiction based therapeutic strategies that aim to select drug targets within the same oncogenic pathway (Luo *et al.*, 2009a,b).

CONCLUSIONS

In summary, in this work we have adapted a known graph theoretical framework for studying dynamics on networks to elucidate a system-omic hallmark of cancer. Specifically, we have shown that the cancer cell phenotype is characterised by an increase in information flux entropy, and that this increase is intricately linked to the network and the dynamics defined on it. Further investigation of the statistical mechanical principles characterising cancer gene networks is warranted as it may help rationalize the choice of drug targets.

ACKNOWLEDGEMENTS

Funding: JW is supported by a CoMPLEX PhD studentship. SS is supported by the Royal Society. AET is supported by a Heller Research Fellowship.

REFERENCES

- Badea, L., Herlea, V., Dima, S. O., Dumitrascu, T., and Popescu, I. (2008). Combined gene expression analysis of whole-tissue and microdissected pancreatic ductal adenocarcinoma identifies genes specifically overexpressed in tumor epithelia. *Hepatology*, **55**(88), 2016–2027.
- Bandyopadhyay, S., Mehta, M., Kuo, D., Sung, M. K., Chuang, R., Jaehnig, E. J., Bodenmiller, B., Licon, K., Copeland, W., Shales, M., Fiedler, D., Dutkowski, J., Gunol, A., van Attikum, H., Shokat, K. M., Kolodner, R. D., Huh, W. K., Aebersold, R., Keogh, M. C., Krogan, N. J., and Ideker, T. (2010). Rewiring of genetic networks in response to dna damage. *Science*, **330**(6009), 1385–1389.
- Barrat, A., Barthelemy, M., and Vespignani, A. (2008). *Dynamical Processes on Complex Networks*. CUP.
- Brin, S. and Page, L. (1998). The anatomy of a large-scale hypertextual web search engine. *Comput Networks and ISDN Systems*, **30**, 107–117.
- Califano, A. (2011). Rewiring makes the difference. *Mol Syst Biol*, **7**, 463.
- Cerami, E. G., Gross, B. E., Demir, E., Rodchenkov, I., Babur, O., Anwar, N., Schultz, N., Bader, G. D., and Sander, C. (2011). Pathway commons, a web resource for biological pathway data. *Nucleic Acids Res*, **39**(Database), D685–D690.
- Chuang, H. Y., Lee, E., Liu, Y. T., Lee, D., and Ideker, T. (2007). Network-based classification of breast cancer metastasis. *Mol Syst Biol*, **3**, 140.
- Chung, F. (2007). The heat kernel as the pagerank of a graph. *PNAS*, **104**(50), 19735–19740.

- Cui, Q., Ma, Y., Jaramillo, M., Bari, H., Awan, A., Yang, S., Zhang, S., Liu, L., Lu, M., O'Connor-McCourt, M., Purisima, E. O., and Wang, E. (2007). A map of human cancer signaling. *Mol Syst Biol*, **3**, 152.
- D'Errico, M., de Rinaldis, E., Blasi, M. F., Viti, V., Falchetti, M., Calcagnile, A., Sera, F., Saieva, C., Ottini, L., Palli, D., Palombo, F., Giuliani, A., and Dogliotti, E. (2009). Genome-wide expression profile of sporadic gastric cancers with microsatellite instability. *Eur J Cancer*, **45**(3), 461–469.
- Estrada, E. and Rodriguez-Velazquez, J. A. (2005). Subgraph centrality in complex networks. *Phys Rev E*, **71**(5).
- Forbes, S. A., Bindal, N., Bamford, S., Cole, C., Kok, C. Y., Beare, D., Jia, M., Shepherd, R., Leung, K., Menzies, A., Teague, J. W., Campbell, P. J., Stratton, M. R., and Futreal, P. A. (2011). Cosmic: mining complete cancer genomes in the catalogue of somatic mutations in cancer. *Nucleic Acids Res*, **39**(Database), D945–D950.
- Hanahan, D. and Weinberg, R. A. (2011). Hallmarks of cancer: the next generation. *Cell*, **144**(5), 646–674.
- Hudson, N. J., Reverter, A., and Dalrymple, B. P. (2009). A differential wiring analysis of expression data correctly identifies the gene containing the causal mutation. *PLoS Comput Biol*, **5**(5), e1000382.
- Ideker, T. and Krogan, N. J. (2012). Differential network biology. *Mol Syst Biol*, **8**, 565.
- Kandasamy, K., Mohan, S. S., Raju, R., Keerthikumar, S., Kumar, G. S., Venugopal, A. K., Telikicherla, D., Navarro, J. D., Mathivanan, S., Pecquet, C., Gollapudi, S. K., Tattikota, S. G., Mohan, S., Padhukasahasram, H., Subbannayya, Y., Goel, R., Jacob, H. K., Zhong, J., Sekhar, R., Nanjappa, V., Balakrishnan, L., Subbaiah, R., Ramachandra, Y. L., Rahiman, B. A., Prasad, T. S., Lin, J. X., Houtman, J. C., Desiderio, S., Renaud, J. C., Constantinescu, S. N., Ohara, O., Hirano, T., Kubo, M., Singh, S., Khatri, P., Draghici, S., Bader, G. D., Sander, C., Leonard, W. J., and Pandey, A. (2010). Netpath: a public resource of curated signal transduction pathways. *Genome Biol*, **11**(1), R3.
- Komurov, K. and Ram, P. T. (2010). Patterns of human gene expression variance show strong associations with signaling network hierarchy. *BMC Syst Biol*, **4**, 154.
- Komurov, K., White, M. A., and Ram, P. T. (2010). Use of data-biased random walks on graphs for the retrieval of context-specific networks from genomic data. *PLoS Comput Biol*, **6**(8).
- Landi, M. T., Dracheva, T., Rotunno, M., Figueroa, J. D., Liu, H., Dasgupta, A., Mann, F. E., Fukuoka, J., Hames, M., Bergen, A. W., Murphy, S. E., Yang, P., Pesatori, A. C., Consonni, D., Bertazzi, P. A., Wacholder, S., Shih, J. H., Caporaso, N. E., and Jen, J. (2008). Gene expression signature of cigarette smoking and its role in lung adenocarcinoma development and survival. *PLoS One*, **3**(2), e1651.
- Lens, S. M., Voest, E. E., and Medema, R. H. (2010). Shared and separate functions of polo-like kinases and aurora kinases in cancer. *Nat Rev Cancer*, **10**(12), 825–841.
- Lucena-Araujo, A. R., de Oliveira, F. M., Leite-Cueva, S. D., dos Santos, G. A., Falcao, R. P., and Rego, E. M. (2011). High expression of aurka and aurkb is associated with unfavorable cytogenetic abnormalities and high white blood cell count in patients with acute myeloid leukemia. *Leuk Res*, **35**(2), 260–264.
- Luo, J., Emanuele, M. J., Li, D., Creighton, C. J., Schlabach, M. R., Westbrook, T. F., Wong, K. K., and Elledge, S. J. (2009a). A genome-wide RNAi screen identifies multiple synthetic lethal interactions with the ras oncogene. *Cell*, **137**(5), 835–848.
- Luo, J., Solimini, N. L., and Elledge, S. J. (2009b). Principles of cancer therapy: oncogene and non-oncogene addiction. *Cell*, **136**(5), 823–837.
- Manke, T., Demetrius, L., and Vingron, M. (2005). Lethality and entropy of protein interaction networks. *Genome Inform*, **16**(1), 159–163.
- Manke, T., Demetrius, L., and Vingron, M. (2006). An entropic characterization of protein interaction networks and cellular robustness. *J R Soc Interface*, **3**(11), 843–850.
- Milanesi, L., Romano, P., Castellani, G., Remondini, D., and Li, P. (2009). Trends in modeling biomedical complex systems. *BMC Bioinformatics*, **10**, 11.
- Morozova, O., Vojvodic, M., Grinshtein, N., Hansford, L. M., Blakely, K. M., Maslova, A., Hirst, M., Cezard, T., Morin, R. D., Moore, R., Smith, K. M., Miller, F., Taylor, P., Thiessen, N., Varhol, R., Zhao, Y., Jones, S., Moffat, J., Kislinger, T., Moran, M. F., Kaplan, D. R., and Marra, M. A. (2010). System-level analysis of neuroblastoma tumor-initiating cells implicates aurkb as a novel drug target for neuroblastoma. *Clin Cancer Res*, **16**(18), 4572–4582.
- Nibbe, R. K., Koyutrk, M., and Chance, M. R. (2010). An integrative -omics approach to identify functional sub-networks in human colorectal cancer. *PLoS Comput Biol*, **6**(1), e1000639.
- Park, H. S., Park, W. S., Bondaruk, J., Tanaka, N., Katayama, H., Lee, S., Spiess, P. E., Steinberg, J. R., Wang, Z., Katz, R. L., Dinney, C., Elias, K. J., Lotan, Y., Naeem, R. C., Baggerly, K., Sen, S., Grossman, H. B., and Czerniak, B. (2008). Quantitation of aurora kinase a gene copy number in urine sediments and bladder cancer detection. *J Natl Cancer Inst*, **100**(19), 1401–1411.
- Platzer, A., Perco, P., Lukas, A., and Mayer, B. (2007). Characterization of protein-interaction networks in tumors. *BMC Bioinformatics*, **8**, 224.
- Prasad, T. S., Kandasamy, K., and Pandey, A. (2009). Human protein reference database and human proteinpedia as discovery tools for systems biology. *Methods Mol Biol*, **577**, 67–79.
- Pujana, M. A., Han, J. D., Starita, L. M., Stevens, K. N., Tewari, M., Ahn, J. S., Rennert, G., Moreno, V., Kirchhoff, T., Gold, B., Assmann, V., Elshamy, W. M., Rual, J. F., Levine, D., Rozek, L. S., Gelman, R. S., Gunsalus, K. C., Greenberg, R. A., Sobhian, B., Bertin, N., Venkatesan, K., Ayivi-Guedehoussou, N., Sol, X., Hernandez, P., Lzaro, C., Nathanson, K. L., Weber, B. L., Cusick, M. E., Hill, D. E., Offit, K., Livingston, D. M., Gruber, S. B., Parvin, J. D., and Vidal, M. (2007). Network modeling links breast cancer susceptibility and centrosome dysfunction. *Nat Genet*, **39**(11), 1338–1349.
- Rhodes, D. R., Yu, J., Shanker, K., Deshpande, N., Varambally, R., Ghosh, D., Barrette, T., Pandey, A., and Chinnaiyan, A. M. (2004). Large-scale meta-analysis of cancer microarray data identifies common transcriptional profiles of neoplastic transformation and progression. *Proc Natl Acad Sci U S A*, **101**(25), 9309–9314.
- Sanchez-Carbayo, M., Socci, N. D., Lozano, J., Saint, F., and Cordon-Cardo, C. (2006). Defining molecular profiles of poor outcome in patients with invasive bladder cancer using

- oligonucleotide microarrays. *J Clin Oncol*, **24**(5), 778–789.
- Schaefer, J. and Strimmer, K. (2005). An empirical bayes approach to inferring large-scale gene association networks. *Bioinformatics*, **21**(6), 754–764.
- Schramm, G., Nandakumar, K., and Konig, R. (2010). Regulation patterns in signaling networks of cancer. *BMC Syst Biol*, **4**(1), 162.
- Scotto, L., Narayan, G., Nandula, S. V., Arias-Pulido, H., Subramaniam, S., Schneider, A., Kaufmann, A. M., Wright, J. D., Pothuri, B., Mansukhani, M., and Murty, V. V. (2008). Identification of copy number gain and overexpressed genes on chromosome arm 20q by an integrative genomic approach in cervical cancer: potential role in progression. *Genes Chromosomes Cancer*, **47**(9), 755–765.
- Smyth, G. K. (2004). Linear models and empirical bayes methods for assessing differential expression in microarray experiments. *Stat Appl Genet Mol Biol*, **3**, Article3.
- Subramanian, A., Tamayo, P., Mootha, V. K., Mukherjee, S., Ebert, B. L., Gillette, M. A., Paulovich, A., Pomeroy, S. L., Golub, T. R., Lander, E. S., and Mesirov, J. P. (2005). Gene set enrichment analysis: a knowledge-based approach for interpreting genome-wide expression profiles. *Proc Natl Acad Sci U S A*, **102**(43), 15545–15550.
- Taylor, I. W., Linding, R., Warde-Farley, D., Liu, Y., Pesquita, C., Faria, D., Bull, S., Pawson, T., Morris, Q., and Wrana, J. L. (2009). Dynamic modularity in protein interaction networks predicts breast cancer outcome. *Nat Biotechnol*, **27**(2), 199–204.
- TCGA, N. (2011). Integrated genomic analyses of ovarian carcinoma. *Nature*, **474**(7353), 609–615.
- Teschendorff, A. E. and Severini, S. (2010). Increased entropy of signal transduction in the cancer metastasis phenotype. *BMC Syst Biol*, **4**, 104.
- Tieri, P., Grignolio, A., Zaikin, A., Mishto, M., Remondini, D., Castellani, G. C., and Franceschi, C. (2010). Network, degeneracy and bow tie integrating paradigms and architectures to grasp the complexity of the immune system. *Theor Biol Med Model*, **7**, 32.
- Tuck, D. P., Kluger, H. M., and Kluger, Y. (2006). Characterizing disease states from topological properties of transcriptional regulatory networks. *BMC Bioinformatics*, **7**, 236.
- Ulitsky, I. and Shamir, R. (2007). Identification of functional modules using network topology and high-throughput data. *BMC Syst Biol*, **1**, 8.
- van Wieringen, W. N. and van der Vaart, A. W. (2011). Statistical analysis of the cancer cell's molecular entropy using high-throughput data. *Bioinformatics*, **27**(4), 556–563.
- Vazquez, A. (2010). Protein interaction networks. in: Alzate o, editor. *Neuroproteomics*.
- Wood, L. D., Parsons, D. W., Jones, S., Lin, J., Sjöblom, T., Leary, R. J., Shen, D., Boca, S. M., Barber, T., Ptak, J., Silliman, N., Szabo, S., Dezso, Z., Ustyanksky, V., Nikolskaya, T., Nikolsky, Y., Karchin, R., Wilson, P. A., Kaminker, J. S., Zhang, Z., Croshaw, R., Willis, J., Dawson, D., Shipitsin, M., Willson, J. K., Sukumar, S., Polyak, K., Park, B. H., Pethiyagoda, C. L., Pant, P. V., Ballinger, D. G., Sparks, A. B., Hartigan, J., Smith, D. R., Suh, E., Papadopoulos, N., Buckhaults, P., Markowitz, S. D., Parmigiani, G., Kinzler, K. W., Velculescu, V. E., and Vogelstein, B. (2007). The genomic landscapes of human breast and colorectal cancers. *Science*, **318**(5853), 1108–1113.
- Wu, C. F. J. (1986). Jackknife, bootstrap and other resampling methods in regression analysis. In *The Annals of Statistics*, volume 14, pages 1261–1295.
- Wurmbach, E., Chen, Y. B., Khitrov, G., Zhang, W., Roayaie, S., Schwartz, M., Fiel, I., Thung, S., Mazzaferro, V., Bruix, J., Bottinger, E., Friedman, S., Waxman, S., and Llovet, J. M. (2007). Genome-wide molecular profiles of hcv-induced dysplasia and hepatocellular carcinoma. *Hepatology*, **45**(4), 938–947.
- Yao, C., Li, H., Zhou, C., Zhang, L., Zou, J., and Guo, Z. (2010). Multi-level reproducibility of signature hubs in human interactome for breast cancer metastasis. *BMC Syst Biol*, **4**, 151.
- Yu, H., Kim, P. M., Sprecher, E., Trifonov, V., and Gerstein, M. (2007). The importance of bottlenecks in protein networks: correlation with gene essentiality and expression dynamics. *PLoS Comput Biol*, **3**(4), e59.

SUPPLEMENTARY FIGURE LEGENDS

Fig.S1

Comparison of local average Pearson correlation coefficients (PCC) with non-local average PCC. Shown are the densities (y-axis) of the correlation values (x-axis). PCC were computed over normal samples only, for six different tissues as indicated. In the local case, for each node an average over the nearest neighbors in the PIN is computed. In the non-local case (green), for each node the average is computed over a random selection of other nodes in the PIN, and shown are the densities for 10 different randomisations. P-values are from a paired Wilcoxon-rank sum tests testing the difference between the local and non-local distributions.